

Angular Distribution of Gamma Rays from Coulomb Excitation

F. K. MCGOWAN AND P. H. STELSON
Oak Ridge National Laboratory, Oak Ridge, Tennessee
 (Received March 30, 1955)

The angular distributions of gamma rays with respect to the incident proton beam on a thick target have been measured for gamma rays following Coulomb excitation in $Pt^{194,196}$, Au^{197} , Ta^{181} , $Ag^{107,109}$, Pd^{106} , Pd^{108} , Pd^{110} , and Rh^{103} . The observed angular distributions deviate considerably from the semiclassical theory of angular distributions of gamma rays following Coulomb excitation given by Alder and Winther. Empirical curves of energy-dependent coefficients $a_\nu(\xi)$ for a thick target are obtained from the results for $Pt^{194,196}$ and Pd^{106} . With these empirical coefficients, information on the spin sequences and the character of the gamma transitions are deduced from the angular distribution measurements in the odd mass nuclei. The spin sequences are as follows: $7/2(E2)3/2$ and $5/2(E2+M1)3/2$ with $\delta_\gamma = -0.75$ (where $\delta_\gamma^2 = E2/M1$) for the 550- and 277-keV transitions, respectively, in Au^{197} ; $11/2(E2)7/2$ and $11/2(E2+M1)9/2$ with $\delta_\gamma = 0.51$ for the 303- and 166-keV transitions, respectively, in Ta^{181} ; $5/2(E2)1/2$ and $3/2(E2+M1)1/2$ with $\delta_\gamma = -0.19$ or -1.14 for the 427- and 325-keV transitions, respectively, in $Ag^{107,109}$; and $5/2(E2)1/2$ and $3/2(E2+M1)1/2$ with $\delta_\gamma = -0.18$ or -1.17 for the 365- and 305-keV transitions, respectively, in Rh^{103} .

1. INTRODUCTION

ALDER and Winther,¹ using a semiclassical treatment, have derived explicit expressions for the angular distribution of the gamma radiation following Coulomb excitation. They find that the angular distribution of the gamma radiation with respect to the incident particles is similar to the angular correlation between two gamma rays in cascade. The distribution function is

$$W(\theta) = 1 + \sum_\nu A_\nu a_\nu(\xi) P_\nu(\cos\theta), \quad (1)$$

where the coefficients A_ν are the gamma-gamma directional angular correlation coefficients tabulated by Biedenharn and Rose² for the spin sequence $j_1(E2)j(L_2)j_2$ and the j 's are the spins of the target nucleus, the Coulomb excited state, and the final state after gamma-ray emission, respectively. The coefficients $a_\nu(\xi)$ which depend on the excitation process through the parameter ξ have been evaluated by numerical methods for electric quadrupole excitation by Alder and Winther.

Several workers^{3,4} have reported agreement between theory and experiment for the angular distribution of the 303-keV gamma ray of Ta^{181} and the 550-keV gamma ray of Au^{197} . However, our measurements have shown significant deviations from theory. For instance, the energy coefficient $a_2(\xi)$ was observed to be 17 percent smaller than theoretically expected at $E_p = 4.0$ Mev for the 303-keV gamma ray in Ta^{181} on the assumption that the spin sequence is $7/2(E2)11/2(E2)7/2$. The results given in this paper suggest that the apparent agreement between theory and experiment found by the other workers is in part the result of the choice of the incident proton energy used in their experiments.

To further test the theory, the angular distributions

of the gamma rays from Coulomb excited states of spin 2 have been examined. In these cases the spin of the excited state is known from gamma-gamma directional angular correlation measurements whereas the spins for the states of the odd-mass nuclei mentioned above were not known with certainty. The spin sequence $0(E2)2(E2)0$ is particularly suitable because the coefficients A_ν are large. In addition, for the cases that have been examined in these experiments, the gamma-gamma directional angular correlation measurements have shown no observable influence of extranuclear fields. This point is important for proton-gamma angular distribution measurements where a target in the solid state is necessary.

A number of other proton-gamma ray angular distributions have been measured and the results are presented. In cases for which the spin of the Coulomb excited state is known from other measurements, the energy dependent coefficients $a_\nu(\xi)$ for a thick target are tabulated. The observed deviations from theory are rather large. Finally, an interpretation of the results, in combination with the empirically determined energy-dependent coefficients, is discussed.

2. APPARATUS

The ORNL 5.5-Mv Van de Graaff accelerator was used to produce a separated beam of protons. Metallic targets which were thick to protons (the range of the protons being ≤ 100 mg/cm²) but thin for the gamma rays were oriented at 45° with respect to the incident protons. The targets (≤ 100 mg/cm²) were prepared from thin foils or were electrodeposited onto 0.005-inch nickel. For the detection of the gamma rays, a scintillation spectrometer employing a NaI crystal 1.5 inches in diameter and 1 inch thick mounted on a DuMont 6292 photomultiplier was used. In all angular distribution experiments the front face of the crystal was located at distances 10.0 or 13.5 cm from the target. To suppress the characteristic K x-rays from the target produced by the impinging protons by factors of 10^2

¹ K. Alder and A. Winther, Phys. Rev. **91**, 1578 (1953).

² L. C. Biedenharn and M. E. Rose, Revs. Modern Phys. **25**, 729 (1953).

³ Eisinger, Cook, and Class, Phys. Rev. **94**, 735 (1954); **95**, 628(A) (1954); **96**, 658 (1954).

⁴ W. I. Goldburg and R. M. Williamson, Phys. Rev. **95**, 767 (1954).

to 10^3 , a graded shield was placed in front of the NaI detector. The graded shields were as follows: for targets with $Z \geq 78$ the shield consisted of 0.010 inch of Ta plus 0.030 inch of Sn plus 0.005 inch of Cu; for a Ta target the shield consisted of 0.040 inch of Sn plus 0.005 inch of Cu; and for targets with $45 \leq Z \leq 53$ the shield consisted of 0.0035 inch of Mo plus 0.005 inch of Cu. Most of the data in these experiments were recorded automatically at 10° increments from 0° to 90° and from 210° to 270° . The time for the collection of a fixed number of counts was printed on a paper tape by a printing timer and the integrated current was recorded by a traffic counter. The angular positions were changed manually. To assure that the axis of rotation of the detector passed through the target, the following alignment procedure was used. The position at which the proton beam impinged on the target was located. A source of Cs^{137} of the same area as the beam was placed on the target at this position. The axis of rotation was adjusted until counting rates showed that the variation in the solid angle subtended by the detector at the target as a function of angular position was less than 0.5 percent. The position of the beam on the target was observed to remain fixed as a function of the beam energy.

3. DISCUSSION OF METHOD

Angular distribution measurements of the gamma rays were carried out with either a single-channel or a multichannel pulse-height analyzer of the ORNL design. In the measurements with a single channel the window of the analyzer was always operated to include only the full energy pulse spectrum peak of the gamma ray. In the case of the multichannel measurements, the full energy pulse spectrum peak was observed and the area of the peak was taken as a measure of the intensity. After each measurement of the intensity at an angle θ_i the intensity was measured either at $\theta = 90^\circ$ or at $\theta = 0^\circ$. In this way the intensities could be corrected for changes in gain of the detector or fractional acceptance of the window of the single-channel analyzer. In all cases, the intensities have been corrected for the bremsstrahlung continuum by measuring the intensity of the bremsstrahlung as a function of θ_i . For angular distribution measurements involving $Z \geq 73$ a Bi target electro-deposited onto nickel was used and for measurements involving $Z \sim 50$ a tin target was used. Bi and Sn targets are well suited for this purpose because of the absence of gamma rays from Coulomb excitation. We believe the extrapolation to neighboring Z will give little error since our investigations of the bremsstrahlung process show relatively little change in character with a small change in Z . In general for the measurements to be discussed below the intensity of the bremsstrahlung in the angular distributions was never more than a few percent of the gamma-ray intensity from Coulomb excitation. Finally, a correction for the attenuation of the gamma rays in the target and target backing as a function of θ_i

was applied to the observed intensities. If this correction was no larger than 5 percent, a computed attenuation using the absorption cross sections taken from NBS-1003⁵ was applied. If the correction was larger, the attenuation was measured directly by placing a source of gamma radiation of the same energy on the target. A least squares fit of the corrected intensities (with the appropriate weight factors) in terms of a series of Legendre polynomials,

$$W(\theta) = \mathcal{A}_0' + \mathcal{A}_2' P_2(\cos\theta) + \mathcal{A}_4' P_4(\cos\theta), \quad (2)$$

was carried out on an I.B.M. calculator. The standard deviations quoted in Table I have been obtained from Eq. (30) in a paper by Rose.⁶ The values of ϵ^2 , defined by Eq. (27),⁶ clustered about unity indicating that nonstatistical errors were not large. A least-squares fit of each set of data in terms of a series of $\cos^{2n}\theta$ was carried out to serve as a check on the I.B.M. calculations. In Table I we tabulate $(a_\nu A_\nu)_{\text{exp}}$, which have been corrected for finite angular resolution⁶ and are defined as

$$(a_\nu A_\nu)_{\text{exp}} = \mathcal{A}_\nu / \mathcal{A}_0.$$

4. MEASUREMENTS AND RESULTS

A. Pt^{194,196}

From the β decay of Ir¹⁹⁴ and Au¹⁹⁶, the first excited states in Pt¹⁹⁴ and Pt¹⁹⁶ are known to exist at 330 and 358 keV, respectively. Directional angular correlation measurements⁷⁻⁹ have verified the spin assignment of 2 for these excited states.

The differential pulse-height spectrum of the gamma radiation from platinum for $E_p = 5.0$ MeV is shown in an accompanying paper.¹⁰ The proton-gamma angular distribution of the 330- and 358-keV gamma rays taken together has been measured for $E_p = 2.5$ to 5.0 MeV. The results are tabulated in Table I. All entries in Table I represent the mean of several determinations of the angular distribution coefficients. A comparison between theory and experiment is shown in Fig. 1. The solid curves labelled "theory" are the thick target energy-dependent coefficients $(a_\nu)_t$ deduced from the excitation cross section and the thin target coefficients a_ν given by Alder and Winther. A procedure for obtaining $(a_\nu)_t$ will be discussed in Sec. 5. The observed energy dependence of the coefficients for a thick target deviates considerably from the theory.

The second excited states in Pt¹⁹⁴ and Pt¹⁹⁶ are known to have spin 2.^{8,9} If these states were appreciably excited by Coulomb excitation, then the observed proton-gamma angular distribution would be a com-

⁵ G. R. White, National Bureau of Standards Circular NBS-1003, 1952 (unpublished).

⁶ M. E. Rose, Phys. Rev. **91**, 610 (1953).

⁷ J. J. Kraushaar and M. Goldhaber, Phys. Rev. **89**, 1081 (1953).

⁸ R. M. Steffen, Phys. Rev. **89**, 665 (1953).

⁹ Mandeville, Varma, and Saraf, Phys. Rev. **98**, 94 (1955).

¹⁰ P. H. Stelson and F. K. McGowan, preceding paper [Phys. Rev. **99**, 112 (1955)].

TABLE I. Proton-gamma angular distribution coefficients of the terms in the expansion of the correlation function in Legendre polynomials for a thick target.

Nucleus	E_{γ} (keV)	E_p (MeV)	Spin sequence	$(A_2)\gamma\gamma$	$(a_2A_2)_{exp}$	$(a_2)_{exp}$	$(A_4)\gamma\gamma$	$(a_4A_4)_{exp}$	$(a_4)_{exp}$	$(A_6)_{exp}$	$\delta\gamma$
$^{194,196}\text{Pt}$	330 and 358	2.5	0(E2)2(E2)0	0.3571	0.286±0.005	0.800±0.015	1.143	-(0.078±0.010)	-(0.068±0.010)		
		3.0		0.253±0.004	0.709±0.010		-(0.062±0.006)	-(0.054±0.005)			
		3.5		0.227±0.003	0.636±0.008		-(0.026±0.008)	-(0.023±0.007)			
		4.0		0.211±0.003	0.591±0.007		-(0.013±0.004)	-(0.011±0.004)			
		4.5		0.191±0.005	0.535±0.015		-(0.007±0.008)	-(0.006±0.007)			
	5.0		0.171±0.003	0.479±0.008		0.001±0.003	0.001±0.003				
Au^{197}	550	3.5 ^a	3/2(E2)7/2(E2)3/2	0.2186	0.176±0.006	0.80 ±0.03	0.1282	-(0.004±0.008)			
		4.0 ^a		0.161±0.006	0.74 ±0.03		-(0.010±0.008)				
		5.0 ^a		0.123±0.006	0.58 ±0.03		0.010±0.008				
		4.0		0.164±0.004	0.75 ±0.02		-(0.018±0.005)				
Au^{197}	277	4.0	3/2(E2)5/2(E2+M1)3/2		-(0.115±0.004)			0.003±0.005		-(0.21±0.01)	-(0.75±0.20)
Ta^{181}	303	4.0	7/2(E2)11/2(E2)7/2	0.1688	0.089±0.004	0.53 ±0.02	0.0500	-(0.006±0.004)			
Ta^{181}	166	4.0	7/2(E2)11/2(E2+M1)9/2		0.112±0.006			0.020±0.008		0.21±0.01	0.51 or 3.0
$\text{Ag}^{107,109}$	325	2.5	1/2(E2)3/2(E2+M1)1/2		-(0.282±0.004)			0.007±0.007		-(0.39±0.02)	-0.19 or -1.14
$\text{Ag}^{107,109}$	427	2.5	1/2(E2)5/2(E2)1/2	0.2857	0.248±0.004	0.868±0.015	0.3809	-(0.039±0.009)	-(0.102±0.024)		
Pd^{110}	380	2.1	0(E2)2(E2)0	0.3571	0.285±0.008	0.80 ±0.02	1.143	-(0.088±0.011)	-(0.077±0.010)		
	2.5			0.243±0.006	0.68 ±0.02		-(0.032±0.008)	-(0.028±0.007)			
	2.5			0.270±0.004	0.75 ±0.01		-(0.050±0.007)	-(0.044±0.007)			
	2.9			0.211±0.006	0.59 ±0.02		-(0.005±0.010)	-(0.005±0.009)			
Pd^{108}	445	2.5	0(E2)2(E2)0	0.3571	0.255±0.009	0.72 ±0.03	1.143	-(0.071±0.008)	-(0.062±0.007)		
Pd^{106}	520	2.1	0(E2)2(E2)0	0.3571	0.343±0.007	0.96 ±0.02	1.143	-(0.143±0.010)	-(0.125±0.009)		
	2.5			0.315±0.007	0.88 ±0.02		-(0.092±0.010)	-(0.080±0.009)			
	2.5			0.340±0.005	0.95 ±0.02		-(0.107±0.018)	-(0.094±0.017)			
	2.9			0.279±0.006	0.78 ±0.02		-(0.065±0.008)	-(0.057±0.008)			
Rh^{103}	305	1.7	1/2(E2)3/2(E2+M1)1/2		-(0.346±0.006)			0.006±0.007		-(0.380)	
		2.1			-(0.307±0.005)			0.024±0.006		-(0.394)	
		2.5			-(0.274±0.004)			0.019±0.006		-(0.400)	
		2.5			-(0.255±0.004)			0.007±0.004		-(0.372)	
		2.9			-(0.234±0.003)			0.012±0.004		-(0.377)	
Rh^{103}	365	1.7	1/2(E2)5/2(E2)1/2	0.2857	0.288±0.007	1.01 ±0.02	0.3809	-(0.046±0.009)	-(0.121±0.024)		
	2.1			0.247±0.005	0.87 ±0.02		-(0.021±0.006)	-(0.055±0.016)			
	2.5			0.224±0.004	0.78 ±0.01		-(0.027±0.005)	-(0.071±0.013)			
	2.5			0.227±0.003	0.79 ±0.01		-(0.023±0.004)	-(0.060±0.011)			
	2.5		0.200±0.002	0.70 ±0.01		-(0.012±0.003)	-(0.032±0.007)				

^a Thin target (10.5 mg/cm²).

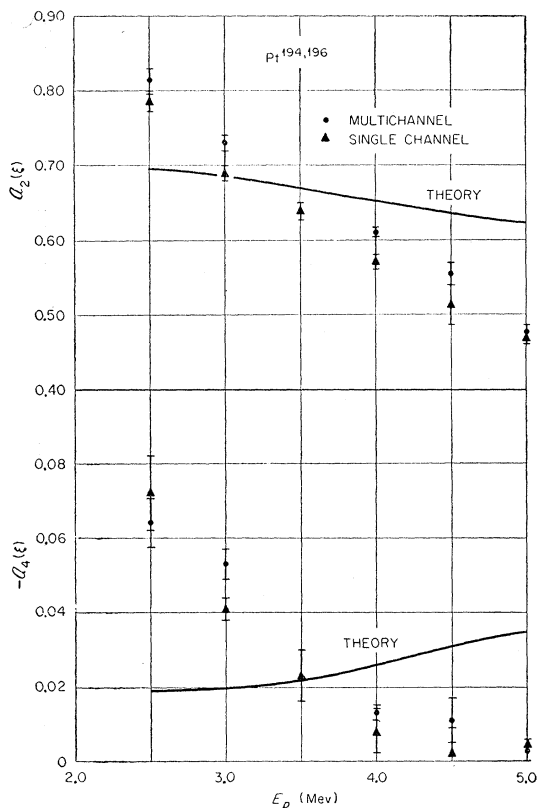


FIG. 1. Thick-target energy-dependent coefficients deduced from the angular distribution measurements of the 330-keV and 358-keV gamma rays from Pt^{194} and Pt^{196} as a function of the incident proton energy. The curves labeled "theory" are the thick-target energy-dependent coefficients deduced from the total cross section for excitation and the thin-target coefficients given by Alder and Winther.

posite angular distribution function. Any significant excitation of the second excited states can be excluded in these isotopes for the following reasons. Recent measurements by Johns and Nablo¹¹ indicate that the second excited state is at 620 keV in Pt^{194} . The intensity ratio of the cascade gamma ray to the cross-over gamma ray is 3. From the differential pulse-height distribution of the gamma radiation resulting from 4.5-MeV protons incident on a thick platinum target we find that the excitation of the 620-keV state in Pt^{194} relative to the direct excitation of the 330-keV state is less than 3 percent. The contribution of 330-keV gamma rays resulting from excitation of the second excited state to the observed angular distribution function is less than 2 percent.

In Pt^{196} , the second excited state is at 688 keV and decays 99 percent of the time by a cascade gamma ray of 330 keV which is 95 percent $E2$ radiation and 5 percent $M1$ radiation.⁸ Assuming the reduced transition probability for excitation of the 688-keV and 358-keV levels are equal, the yield of 330-keV gamma rays by

the cascade transition in Pt^{196} relative to 330- and 358-keV gamma rays would be 5, 7, 10, and 13 percent at $E_p = 3.5, 4.0, 4.5,$ and 5.0 MeV, respectively. However, the reduced transition probability for the 358-keV transition in Pt^{196} is 20 times larger than independent particle theoretical estimate [see Eq. (VII. 9) given by Bohr and Mottelson].¹² Consequently, the assumption made above, i.e., that the reduced transition probability for excitation of the 682-keV state is equal to that for the 358-keV state, requires the reduced transition probability for the 330-keV cascade to be 4×10^3 times larger than the independent particle estimate and this seems rather unlikely.

B. Au^{197}

The proton-gamma angular distributions of the 550-keV and 277-keV gamma rays in Au^{197} have been measured by several workers.^{3,4} Spins of $7/2$ and $5/2$ for the 550-keV and 277-keV levels, respectively, were deduced from their measurements. For the 277-keV transition Goldberg and Williamson,⁴ and Eisinger *et al.*³ obtained $E2/M1 = 0.07$ and 0.59 , respectively, by applying the energy-dependent coefficients a_ν given by Alder and Winther to their angular distribution measurements. Measurements of the proton-gamma angular distributions have been carried out for the 550-keV gamma ray in Au^{197} using thick and thin targets and for the 277-keV gamma ray in Au^{197} using a thick target. The thin target was prepared by spot-welding a thin Au foil on a Bi backing which was electrodeposited on nickel. The Bi backing served as a catcher for the protons emerging from the Au target. The results of the measurements are tabulated in Table I. The measurements for the 277-keV radiation have been treated as entirely the result of direct excitation of 277-keV level. The cascade radiation (273-, 277-keV γ rays) from the 550-keV level contributes about 4 percent to the intensity of 277-keV gamma radiation¹⁰ at $E_p = 4.0$ MeV.

C. Ta^{181}

The proton-gamma angular distribution of the 303-keV gamma ray in Ta^{181} has been measured by several workers^{3,4} and a spin of $11/2$ for the 303-keV level was deduced from their measurements. In addition to measurements of the proton-gamma angular distribution of the 303-keV gamma ray we have measured the proton-gamma angular distribution of the 166-keV cascade gamma ray from the 303-keV state. For the latter measurements, the window of the analyzer was set on the high energy edge of the 166-keV full pulse spectrum peak in order to exclude the detection of 137-keV gamma radiation. The results of the measurements are tabulated in Table I.

¹¹ M. W. Johns and S. V. Nablo, *Phys. Rev.* **96**, 1599 (1954).

¹² A. Bohr and B. R. Mottelson, *Kgl. Danske Videnskab. Selskab, Mat.-fys. Medd.* **27**, No. 16 (1953).

D. Ag^{107,109} and Rh¹⁰³

Proton-gamma angular distribution measurements have been carried out for the gamma rays in Ag^{107,109} at $E_p=2.5$ Mev using thick targets of normal silver and for two gamma rays in Rh¹⁰³ at $E_p=1.7$ to 2.9 Mev using thick targets. Since the completion of our distribution measurements, Heydenburg and Temmer¹³ have reported that the two corresponding excited states in Ag¹⁰⁷ and Ag¹⁰⁹ differ by only a few kev. As a result the measurements for Ag^{107,109} tabulated in Table I represent angular distribution coefficients of a composite angular distribution function. A comparison of the results with the observed angular distributions for the two gamma rays of Rh¹⁰³ indicates that the angular distribution coefficients for Ag^{107,109} are meaningful, i.e., the spins of the corresponding Coulomb excited states in Rh¹⁰³, Ag¹⁰⁷, and Ag¹⁰⁹ and the character of the gamma radiation are the same.

E. Pd

Proton-gamma angular distributions have been carried out for the 445-kev gamma ray at $E_p=2.5$ Mev and for the 380-kev and 520-kev gamma rays at $E_p=2.1$ to 2.9 Mev using thick targets of palladium. A differential pulse-height spectrum of the gamma radiation from palladium produced by Coulomb excitation is shown in the accompanying paper.¹⁰ The results of measurements are tabulated in Table I. The 520-kev gamma ray is attributed to Pd¹⁰⁶ resulting from the decay of the well-known 513-kev level observed in the β -decay of Rh¹⁰⁶. From gamma-gamma directional angular correlation measurements the spins of the first and second excited states of Pd¹⁰⁶ are known to be 2 and 0, respectively, and the angular correlation measurements are not disturbed by extranuclear fields.¹⁴ The very short lifetime¹⁰ of the intermediate state deduced from the reduced transition probability for excitation of the first excited state in Pd¹⁰⁶ lends support to this latter statement. The second excited state in Pd¹⁰⁶ is, of course, not excited by Coulomb excitation. As a result the angular distribution measurements of the 520-kev gamma ray serve to test the angular distribution theory for medium weight nuclei.

5. DISCUSSION OF RESULTS

In order to compare experimental angular distribution coefficients for a thick target with theory, we must evaluate the expected thick target coefficients. Now, Alder and Winther^{1,15} have given both the total excitation cross section and the angular distribution of the gamma rays with respect to the incident protons for excitation by the electric quadrupole field. The differ-

ential cross section at a given energy E is

$$d\sigma(E)/d\Omega = \sigma(E)W(\theta), \quad (3)$$

where

$$\sigma(E) = \frac{4\pi^2 m B(E2)}{25Z_2^2 e^2 \hbar^2} E_f g_2(\xi)$$

and $W(\theta)$ is given by Eq. (1). For the differential cross section from a thick target for an incident proton energy E_i in the laboratory system, we have

$$\frac{d\sigma(E_i)}{d\Omega} \propto \int_0^{E_i} \frac{\sigma(E)W(\theta)dE}{dE/d\rho x}. \quad (4)$$

We therefore have that the expected coefficient of the Legendre polynomial P_ν for a thick target is given by

$$\frac{\alpha_\nu(E_i)}{\alpha_0(E_i)} = A_\nu \int_0^{E_i} \frac{\sigma(E)a_\nu(E)dE}{dE/d\rho x} / \int_0^{E_i} \frac{\sigma(E)dE}{dE/d\rho x}, \quad (5)$$

or the thick target energy-dependent coefficient is

$$[a_\nu(E_i)]_t = \frac{1}{A_\nu} \frac{\alpha_\nu(E_i)}{\alpha_0(E_i)}. \quad (6)$$

Now let us change from E to the variable ξ , where

$$\xi = \frac{Z_1 Z_2 e^2}{\hbar} \left(\frac{1}{v_f} - \frac{1}{v_i} \right). \quad (7)$$

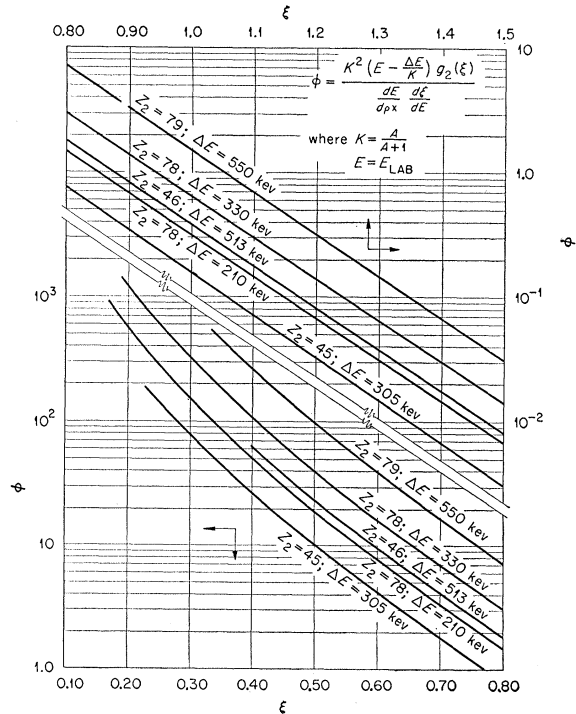


FIG. 2. The function ϕ for representative cases plotted as a function of ξ .

¹³ N. P. Heydenburg and G. M. Temmer, Phys. Rev. **95**, 861 (1954).

¹⁴ E. D. Klema and F. K. McGowan, Phys. Rev. **92**, 1469 (1953).

¹⁵ K. Alder and A. Winther, Phys. Rev. **96**, 237 (1954).

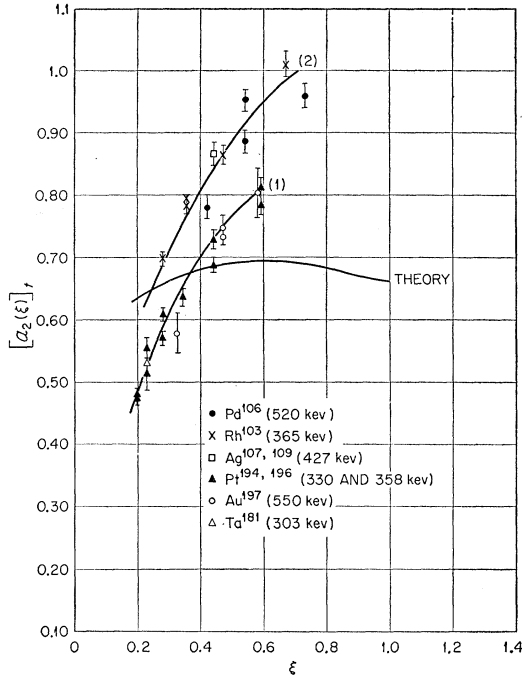


FIG. 3. Thick-target energy-dependent coefficient $a_2(\xi)$ deduced from angular distribution measurements plotted at a value of ξ corresponding to the incident proton energy on the thick target. The solid curve labelled "theory" represents the thick-target energy-dependent coefficient $[a_2(\xi_i)]_t$ as given by Eq. (9).

For any given case we have

$$[a_\nu(\xi_i)]_t = \int_0^{\xi_i} \frac{\sigma a_\nu d\xi}{dE/d\rho x d\xi/dE} / \int_0^{\xi_i} \frac{\sigma d\xi}{dE/d\rho x d\xi/dE} \quad (8)$$

Now for the cases of interest it is found that the energy-dependent part of

$$\frac{\sigma}{dE/d\rho x d\xi/dE}$$

which we shall call ϕ , where

$$\phi = \frac{K^2(E - \Delta E/K)g_2(\xi)}{dE/d\rho x d\xi/dE}$$

as a function of ξ has very nearly the same shape for different Z_2 and ΔE . In Fig. 2, ϕ has been plotted as a function of ξ for representative cases, namely; $\Delta E = 200$ to 550 keV and incident proton energies of practical interest. We then have

$$[a_\nu(\xi_i)]_t = \int_0^{\xi_i} \phi a_\nu(\xi) d\xi / \int_0^{\xi_i} \phi d\xi \quad (9)$$

Thus, according to the theory of Alder and Winther, it follows that $[a_\nu(\xi_i)]_t$ vs ξ_i will be nearly an unique function. Or to put it differently, if many different cases

are measured one would expect the resulting points $a_\nu(\xi_i)_{\text{exp}}$ to fall on a smooth curve as a function of ξ_i .

A comparison between theory and experiment is shown in Figs. 3 and 4 for the cases of $\text{Pt}^{194,196}$ and Pd^{106} where the spin of the Coulomb excited state is known with reasonable certainty. The solid curves labelled "theory" represent the expected thick target energy-dependent coefficient $[a_\nu(\xi_i)]_t$ given by Eq. (9) using for a_ν the numerical calculations of Alder and Winther. For Pd^{106} , the deviations of the observed energy-dependent coefficients from theory for a thick target are even larger than they are for $\text{Pt}^{194,196}$. In addition the coefficient $a_2(\xi_i)_{\text{exp}}$ seems to have a Z_2 dependence over and above that contained in the parameter ξ .

The effect of multiple scattering of the protons by Rutherford scattering as they traverse a thick target on the angular distribution coefficient $[a_\nu(\xi_i)]_t$ should be discussed. Let us consider a proton-gamma angular distribution experiment, where $W(\theta_1)$ is the correlation function and $F(\theta')$ is the multiple scattering function due to Rutherford scattering. The probability that any proton from the collimated incident beam is multiple scattered through an angle θ' in the target prior to a nuclear excitation and that the resulting gamma ray is correlated to the multiple scattered proton by $W(\theta_1)$ is

$$P = \int d\Omega_1 W(\theta_1) F(\theta'). \quad (10)$$

Goudsmit and Saunderson¹⁶ have already expressed the multiple Rutherford scattering function as a series in Legendre polynomials for the case of electrons. Their treatment is exact if one considers electrons with the same total path length in the scatterer. Thus, the coef-

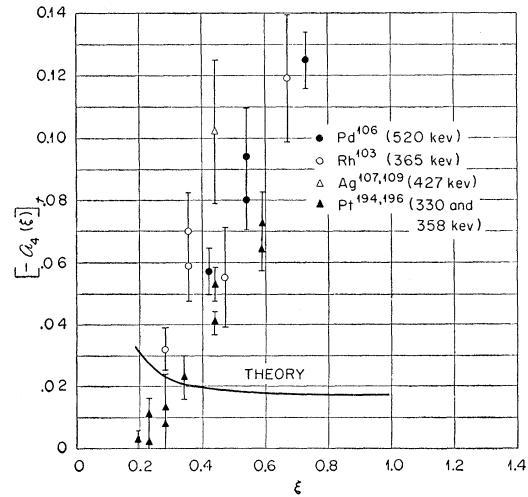


FIG. 4. Thick-target energy-dependent coefficient $a_4(\xi)$ deduced from angular distribution measurements plotted at a value of ξ corresponding to the incident proton energy on the thick target. The solid curve labelled "theory" represents the thick-target energy-dependent coefficient $[a_4(\xi_i)]_t$ as given by Eq. (9).

¹⁶ S. Goudsmit and J. L. Saunderson, Phys. Rev. **57**, 24 (1940).

ficients G_k (coefficients of the Legendre polynomials representing the multiple Rutherford scattering function) given by Goudsmit and Saunderson should be applicable to the case of protons. A solution of this problem on the effect of multiple scattering on the proton-gamma angular distribution is similar to the effect of scattering of electrons in a conversion electron-gamma angular distribution.¹⁷ The form of the correlation function is unchanged and each coefficient $a_n A_n$ becomes multiplied by an attenuation factor G_p . We have evaluated the effect of multiple scattering on the thick target angular distribution coefficients by replacing $a_n(\xi)$ in Eq. (9) by $a_n(\xi)G_p$ and considering the case $a_n(\xi)$ is constant. The results are tabulated in Table II. The effect of multiple Rutherford scattering on the observed thick target energy-dependent coefficients is in the right direction but is not nearly large enough to account for the difference between curves (1) and (2) of Fig. 3. In any case the attenuation coefficients for multiple scattering are significant and should be included in the analysis of thick target angular distribution measurements. The coefficients in Table I have not been corrected for multiple Rutherford Scattering because we have no satisfactory thin target a_n from which we could evaluate these attenuation coefficients for a thick target.

Since the deviations between theory and experiment appears to be rather large, we have chosen to analyze the remainder of the data in Table I using empirically determined energy dependent coefficients from a plot of $a_n(\xi_i)_{\text{exp}}$ vs ξ_i . For neighboring nuclei this method of presenting the data appears to be useful. Of the possible spin sequences that need to be considered for the 550-keV and 303-keV gamma rays in Au¹⁹⁷ and Ta¹⁸¹, respectively, on the assumption that the radiation is E2, only the spin sequences suggested originally by Eisinger *et al.*³ and by Goldberg and Williamson⁴ yield energy dependent coefficients $a_2(\xi_i)_{\text{exp}}$ that agree with the empirical $[a_2(\xi_i)]_t$ given in Fig. 3. These additional coefficients determined from the Au¹⁹⁷ and Ta¹⁸¹ data are tabulated in Table I and are plotted in Fig. 3.

In general, for odd mass nuclei, the radiation from the first Coulomb excited state and the cascade radiation from the second Coulomb excited state will be $E2+M1$ radiation. In addition to inferring the spin of the excited states, information on the ratio of the quadrupole to dipole intensity is obtained from angular distribution measurements. We have applied the empirical $[a_2(\xi_i)]_t$ to our data for Au¹⁹⁷ and Ta¹⁸¹ and for the indicated spin sequence in Table I. From the tabulated $(A_2)_{\text{exp}}$ for the 277-keV transition in Au¹⁹⁷ one finds $\delta_\gamma = -(0.75 \pm 0.20)$ where δ_γ^2 is the ratio of the squares of the reduced matrix elements² and is defined as the intensity ratio (in this case) of quadrupole to dipole radiation in the gamma-ray transition. The large uncertainty in δ_γ results from the fact that

TABLE II. Attenuation coefficients for multiple Rutherford scattering for proton-gamma angular distributions from thick targets for the case $a_n(\xi)$ is constant.

Pt^{194} $E_p(\text{Mev})$	$\Delta E = 330 \text{ keV}$		Rh^{103} $E_p(\text{Mev})$	$\Delta E = 365 \text{ keV}$	
	\bar{G}_2	\bar{G}_4		\bar{G}_2	\bar{G}_4
5.0	0.955	0.841	2.9	0.980	0.940
4.0	0.961	0.872	2.5	0.982	0.946
3.0	0.971	0.916	2.1	0.985	0.956
2.0	0.988	0.961	1.7	0.989	0.969

A_2 has a broad maximum at $\delta = -0.75$. This value of δ_γ^2 is in good agreement with that deduced from K -shell internal conversion coefficient measurements.¹⁸ The data for the 166-keV transition in Ta¹⁸¹ lead to $\delta_\gamma = 0.51$ or 3.0. The former value agrees with the δ_γ^2 deduced from a K/L ratio measurements.¹⁹ This sign and magnitude of δ_{166} is identical to δ_{137} of the 137-keV transition in Ta¹⁸¹.²⁰

Huus and Lunden²¹ have suggested spin assignments for the Coulomb excited states in Ag^{107,109} from the position of the levels using the nuclear model of Bohr and Mottelson.¹² Heydenburg and Temmer¹³ have reached similar conclusions for Ag^{107,109} and Rh¹⁰³. The signs of the angular distribution coefficients $(a_2 A_2)_{\text{exp}}$ in Table I fix the level order as 1/2, 3/2, and 5/2 independent of a nuclear model. The angular distribution data for the 427-keV and 365-keV transitions in Ag^{107,109} and Rh¹⁰³, respectively, yield additional determinations of $a_n(\xi_i)$ for a thick target and are plotted in Figs. 3 and 4. These additional data are in good agreement with the empirical curve deduced from the proton-gamma angular distribution measurements of Pd¹⁰⁶. Using these empirical data the spins of the 325-keV and 305-keV states in Ag^{107,109} and Rh¹⁰³, respectively, and the character of the radiation are deduced from the angular distribution data. Actually, the observed angular distributions are composite functions, namely: proton-gamma angular distribution function for the direct excitation of the 325-keV or 305-keV levels and the proton-gamma angular distribution function for 325-keV or 305-keV gamma rays by excitation of the 427-keV and 365-keV levels and not observing the cascade transitions. This latter distribution function is not known explicitly, although we do know approximately what fraction of the observed 325-keV and 305-keV gamma rays result from direct Coulomb excitation of the 325- and 305-keV levels.¹⁰ For the 325-keV transition in Ag^{107,109} about 96 percent of the gamma rays observed are the result of direct Coulomb excitation of the 325-keV level. If we assume that the reduced $E2$ transition probabilities for the 65- and 365-keV transitions in Rh¹⁰³ are equal, then the cascade transition must be predominantly $M1$ ($E2/M1 = 0.002$) or 86 to 92 percent of the 305-keV

¹⁸ Huber, Halter, Joly, Maeder, and Brunner, *Helv. Phys. Acta* **26**, 591(A) (1953).

¹⁹ T. Huus and J. H. Bjerregaard, *Phys. Rev.* **92**, 1579 (1953).

²⁰ F. K. McGowan, *Phys. Rev.* **93**, 471 (1954).

²¹ T. Huus and A. Lunden, *Phil. Mag.* **45**, 966 (1954).

¹⁷ S. Frankel, *Phys. Rev.* **83**, 673 (1951).

gamma rays result from direct Coulomb excitation of the 305-keV level. In the absence of any additional information, we have treated the data as resulting from the direct Coulomb excitation of the 305-keV level. The constancy of $(A_2)_{\text{exp}}$ for different E_p for the 305-keV transition in Rh^{103} probably indicates that the distribution functions entering into the composite function are nearly alike.

In the treatment of the angular distribution data for the 380-keV and 445-keV gamma rays in Pd we assume that the transitions are in ${}_{46}\text{Pd}^{110}$ and ${}_{46}\text{Pd}^{108}$, respectively, as was done in the analysis of the yield data.¹⁰ The trend of $B(E2)/e^2$ with neutron number indicated that the transitions are predominantly in these isotopes. The angular distributions indicate that transitions are predominantly of the type $2(E2)0$. The empirical coefficients $(a_2)_{\text{exp}}$ for these transitions are slightly smaller (the coefficients $(a_2)_{\text{exp}}$ for the 445-keV transition are more so than for the 380-keV transition) than those in Fig. 3 for Pd^{106} , $\text{Ag}^{107,109}$, and Rh^{103} . This is not surprising since we have not attributed any of the gamma rays to Coulomb excitation of Pd^{105} (22.23 percent).

6. CONCLUSIONS

The coefficients $a_\nu(\xi)$ are found to deviate considerably from those given by the semiclassical theory of the process. The fact that the points for heavy (or for medium weight) nuclei fall on a smooth curve indicates that the parameter ξ correctly takes into account the excitation energy and the exciting proton energy. However, from the fact that two distinct curves are obtained we conclude that the dependence on Z_2 is not correctly accounted for. Recently, Biedenharn and Class²² have obtained an exact result for the particular case of no

²² L. C. Biedenharn and C. M. Class, Phys. Rev. **98**, 691 (1955).

energy loss ($\xi=0$). The behavior of a_2 for this special case as a function of the parameter $\eta=Z_1Z_2e^2/\hbar v$ shows appreciable deviations from the classical limit. It is clear that more accurate calculations of the angular distribution coefficients a_ν are needed. Inferring spins of Coulomb excited states using a nuclear model is not very satisfying. One would prefer to arrive at the spins more directly from angular distribution measurements.

For pure multipole radiation from heavy nuclei, one might deduce the correct spin assignment from the existing calculations by Alder and Winther. However, for the medium weight nuclei the deviations between experiment and theory are larger and the deduction of the correct spin assignment would be less certain. In odd-mass nuclei, the radiation from the first Coulomb excited state and the cascade radiation from the second Coulomb excited state will in general be $E2+M1$ radiation. In addition to inferring the spin of the excited states, information on the ratio $E2/M1$ can be determined from the angular distribution measurements. A determination of this ratio demands an accurate knowledge of the coefficients a_ν .

From the results discussed in this paper, it appears possible to use empirically determined energy-dependent coefficients a_ν for a thick target to interpret angular distribution measurements involving pure or mixed multipole transitions in neighboring odd-mass nuclei.

ACKNOWLEDGMENTS

It is a pleasure to express our appreciation to Dr. M. E. Rose and Dr. L. C. Biedenharn for several stimulating discussions concerning the results. We should like to express appreciation to Buford Carter, who carried out the I.B.M. calculations and to Dr. M. H. Lietzke of the Chemistry Division for advice on the electrodeposition of bismuth.